ISSN 0023-1584, Kinetics and Catalysis, 2006, Vol. 47, No. 6, pp. 891–900. © MAIK "Nauka/Interperiodica" (Russia), 2006.
Published in Russian in Kinetika i Kataliz, 2006, Vol. 47, No. 6, pp. 918–928.

Long-Term Deactivation of Pt/Alumina Catalyst by Organosilicons in the Total Oxidation of Hydrocarbons[1]

M. Rahmani* and M. Sohrabi

Chemical Engineering Department, Amirkabir University of Technology, Tehran 15914, Iran

**e-mail: mrahmani@ftml.net*

Received May 15, 2006

Abstract—The deactivation of a supported platinum catalyst by long-term exposure to hexamethyldisiloxane was investigated. Ethyl acetate containing several tenfold excess of organosilicon relative to the real application was fed to the reactor. Three sets of catalyst and the blank support were aged for 350, 650, and 1000 h. The ex situ activity measurements on the aged pellets showed that all samples were deactivated as they were exposed to hexamethyldisiloxane. Silicon species were found at the surfaces of both the catalyst and the blank support. The quantitative analysis of silicon loading showed a linear profile versus poison exposure time and axial position in the bed. The radial silicon distribution in an individual pellet revealed an eggshell distribution of silicon residues, which is an indication of a diffusion-limited mechanism of silicon deposition. The deactivation was attributed to deposition of thin layer of silicon residues, which blocks the surface sites.

DOI: 10.1134/S0023158406060127

1. INTRODUCTION

Supported noble metal catalysts are widely used in air pollution control systems. A major limitation imposed on the reliable operation and useful lifetime of such catalysts is their activity loss by minute amounts of certain species in the feed stream. While chlorine [1], sulfur [1, 2], lead, and phosphorus [3] have been frequently reported as poisons of Pt/alumina catalysts, there are few open literature sources reporting silicon compounds as a deactivating agent.

Organosilicons have a broad range of applications in different industries such as printing, coating and polishing, petroleum extraction, and mining. They are also used in industrial lubricants, silicon polymers, silicon rubbers, and aerosol sprays. These compounds are recognized as poisons/inhibitors in catalytic processes such as total oxidation of volatile organic compounds [4–8], catalytic sensors for detecting flammable gases [9–12], hydrotreating [13], and naphtha reforming [14].

Gentry and Jones [4] have reported the influence of hexamethyldisiloxane (HMDS) on the catalytic oxidation of methane, propene, carbon monoxide, and hydrogen on platinum and palladium with different types of support. They found that HMDS affected the oxidation of each compound differently. Methane oxidation at 600°C over Pt/γ-Al_2O_3 was totally poisoned and the activity fell exponentially to zero. By removing the poison from the feed, the activity was not restored. Passing HMDS vapor during hydrogen and propene oxidation at 600°C on Pt/γ-Al_2O_3 caused a negligible effect on hydrogen oxidation, but revealed a reversible behavior for propene oxidation. A similar observation has been reported for methane and butane oxidation over supported palladium catalysts at 527°C [5]. It was found that the catalysts were almost irreversibly poisoned during the methane oxidation but that they generally recovered much of their activity in oxidation of butane. Examining the long-term field deactivated Pt-Pd/alumina catalysts in a flexography printing application revealed the deposition of silica particles in the catalyst micropores [6]. A steep silicon profile along the bed was observed. Laboratory activity evaluations using hexane showed that the activation energy for the aged catalysts was the same as that for the fresh catalysts. It was suggested that the silica deposition is nonselective and the silica masks the noble metal active sites. In several cases, deactivation of catalytic methane sensors by organosilicons has been described by silica overlayer formation [10–12]. It has been postulated that poisoning effects of HMDS on platinum ribbons is due to the dissociative adsorption of HMDS on the surface.

A rather well covered review on deactivation effects of organosilicon and organophosphorous compounds on oxidation catalysts for abatement of volatile organic compounds has recently been published [15].

The present work examines the influence of organosilicons on the activity of Pt/γ-Al_2O_3 catalyst during total oxidation of volatile organic compounds (VOC). Hexamethyldisiloxane (HMDS) was selected as a poison precursor because it is a monomer of the several industrially used silicon oils. Ethyl acetate, as one of the most frequently encountered VOC in industrial environments, represents the VOC model compound. This is while the complete oxidation of ethyl acetate is

[1] The text was submitted by the authors in English.

Table 1. Typical properties of fresh pellets

	γ-Al_2O_3	Pt/γ-Al_2O_3
Shape	Cylindrical	Cylindrical
Diameter	3 mm	3 mm
Average length	12 mm	7 mm
Average packing density	0.55 kg/dm^3	0.55 kg/dm^3
Pt loading	–	0.073 wt %
Average Pt depth	–	~100×10^{-6} m

rather difficult. The study has been conducted in a pilot unit to simulate the long-term effects.

2. EXPERIMENTAL

2.1. Material

High-purity γ-alumina extrudates from SASOL with a surface area in the range of 95–135 m^2/g and a diameter of 3 mm and length of approximately 12 mm were used as the catalyst support. Pure ethyl acetate (98.8%) and pure hexamethyldisiloxane (98+%) supplied by Sigma Aldrich were used.

2.2. Catalyst

The egg-white catalyst was prepared by the sequential impregnation method. In the first step, the alumina support was impregnated for 15 min, using an aqueous solution of hexachloroplatinic acid as precursor for platinum. After that, the solution was removed and the pellets were washed carefully using deionized water.

In the second step, the pellets were placed in a solution of citric acid as the competitive adsorbate for the desired impregnation duration. At the end of this period, the solution was decanted and the pellets were washed with deionized water. In the third step, the pellets were dried and subsequently calcined at 500°C for 1 h. Finally, the catalyst was activated by reduction in a gas mixture of 5 vol % hydrogen in nitrogen. The reduction was performed at 450°C in a flow reactor for 1 h. The detailed descriptions of synthesis may be found elsewhere [16]. Table 1 summarizes the typical properties of the fresh pellets.

2.3. Pilot Unit

The pilot unit for the long-term deactivation, shown schematically in Fig. 1, consisted of four main sections: feeding system, tubular fixed bed reactor, heat exchanger, and control unit. The solution of ethyl acetate and HMDS was continuously injected into the hot air inside vaporizer, which was fed by the air fan (F-1). This stream was then mixed with air at the outlet of air blower (F-2), fed to the heat exchanger (H-2), and, finally, passed through the fixed bed reactor. An electrical heating element was placed at the reactor inlet for the startup and to adjust the feed temperature to the desired value. The fixed bed reactor was integrated with the heat exchanger in a well-insulated box. The reactor was made of stainless steel, consisting of 12 vertical tubes, each 56 mm in internal diameter and 200 mm in height (Fig. 2). Each tube was equipped with a bottom orifice plate to guarantee an even flow distribution over the tubes. Most of the process variables were controlled and monitored by the control unit.

2.4. Slow Deactivation Procedure

The slow deactivation conditions are shown in Table 2. The reactor inlet temperature was 350°C, kept constant throughout the experiment. The total gas feed flow rate was 100 m^3/h. The gas hourly space velocity (GHSV) was 18518 h^{-1}. When steady state conditions were established, a solution of 0.1727 wt % HMDS in ethyl acetate was injected inside the vaporizer into the hot air stream. Each reactor tube was loaded with

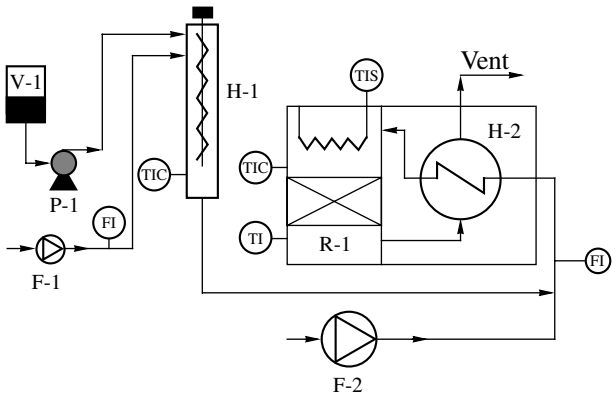

Fig. 1. Schematic flow diagram of pilot unit: (V-1) ethyl acetate + HMDS container, (P-1) dosage pump, (H-1) vaporizer, (F-1) vaporizer fan, (R-1) reactor, (H-2) heat exchanger, (F-2) main air fan.

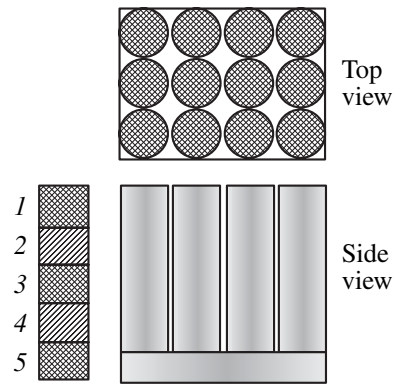

Fig. 2. Schematic diagram of tubular fixed bed reactor.

Table 2. The operating conditions of slow deactivation experiment

At the vaporizer outlet:	
temperature	300°C
normal gas flow rate	2.5 m^3/h
VOC flow rate (Ethyl acetate + HMDS)	100.173 g/h
net flow rate of poison, HMDS	0.173 g/h
At the reactor inlet:	
temperature	350°C
total pressure	1.7 atm (1.717×10^5 Pa)
normal gas flow rate	100 m^3/h
total VOC concentration	1001.73 mg/m^3
HMDS concentration	1.73 mg/m^3
Catalyst loading per tube	450 cm^3
Total Pt/γ-Al_2O_3 loading, 6 tubes	2700 cm^3
Total γ-Al_2O_3 loading, 6 tubes	2700 cm^3
Gas hourly space velocity	18518 h^{-1}, NTP conditions*

* Normal temperature and pressure conditions: 25°C, 1.01×10^5 Pa.

450 cm^3 of pellets. The tubes were divided into five equal sections, separated by a stainless steel mesh. The first, third, and fifth sections (Fig. 2) were designated as the *top*, *middle*, and *bottom* fractions and selected for further analyses.

The slow deactivation was performed in two stages for 350, 650 and 1000 h. The tubes were filled with Pt/γ-Al_2O_3 catalyst (first and third rows, as shown in Fig. 2) and γ-Al_2O_3 (second and fourth rows). After 350 h, the feeding section was brought to a halt, heating was turned off, and the reactor was cooled for 5 h in fresh air. The reactor was then opened and the second and third rows were replaced with fresh samples and the experiment continued for an additional 650 h. By such a procedure, three sets of deactivated catalyst and blank support were finally prepared. One set including three reactor tubes was deactivated for 350 h, one other for 650 h, and the last set for 1000 h.

2.5. Catalytic Activity Measurements

Activity measurements of fresh and deactivated catalysts with respect to pure ethyl acetate were carried out in a laboratory flow reactor described elsewhere [17]. The standard set of operating conditions used for the activity measurements is shown in Table 3. The percent total conversion of ethyl acetate (X) has been calculated as follows:

$$X = \frac{C_{in} - C_{out}}{C_{in}} \times 100. \quad (1)$$

For calculating the total oxidation versus partial oxidation of ethyl acetate, the CO_2 yield is defined according to the following relation:

$$Y = \frac{C_{CO_2}/4}{C_{in}} \times 100, \quad (2)$$

where C_{in} and C_{out} are the concentrations of total hydrocarbons at the reactor inlet and outlet, respectively, and C_{CO_2} is the carbon dioxide concentration at the reactor outlet measured by an IR analyzer.

At low temperatures, owing to the presence of substantial amounts of partial oxidation products, significant differences between X and Y values are apparent. Such differences are reduced as the temperature and, consequently, X are increased. The quality of total oxi-

Table 3. The standard set of operating conditions was used for the activity measurements

Catalyst volume	60 cm^3
Temperature levels	250, 300, 325, 350°C
Pressure	1 atm (1.01×10^5 Pa)
Gas feed flow rate	11.5 l/min (NTP conditions*)
Gas hourly space velocity, GHSV	11500 h^{-1} (NTP conditions*)
Ethyl acetate in the feed	425 ppmv

* Normal temperature and pressure conditions: 25°C, 1.01×10^5 Pa.

Table 4. Surface area and pore structure of fresh and deactivated samples

Catalyst	Deactivation status	Surface area, m^2/g	Pore volume*, cm^3/g
γ-Al_2O_3	Fresh	130	0.68
	350 h, top fraction	119	0.40
	650 h, top fraction	117	0.48
	1000 h, top fraction	113	0.78
Pt/γ-Al_2O_3	Fresh	124	0.77
	350 h, top fraction	118	0.63
	650 h, top fraction	119	0.61
	1000 h, top fraction	118	0.73

*BJH desorption cumulative pore volume.

dation was considered acceptable when the difference between *X* and *Y* values did not exceed 2%.

2.6. Catalyst Characterization

The specific surface area (BET), pore volume, and pore size distribution of the fresh and spent pellets were measured with a Micromeritics ASAP 2010 instrument using adsorption of N_2 at the temperature of liquid nitrogen. Pore volume and pore size distribution in the range of 17–3000 Å were calculated according to BJH method [18]. All the samples were degassed at 200°C in a vacuum for at least 4 h before analysis.

Platinum loading on the fresh catalyst was measured according to ASTM standard D4642-92 using atomic absorption spectrophotometry techniques. The sample was dissolved in hydrochloric acid and gently heated. The absorption of the resulting solution was measured at 403 nm using a Perkin–Elmer spectrophotometer (model Lambda 12).

Scanning electron microscopy (SEM) measurements were conducted using a LEO Gemini 1550 microscope. Samples of the fresh and the spent catalyst were cut radially and their cross sections were scanned without prior surface treatment.

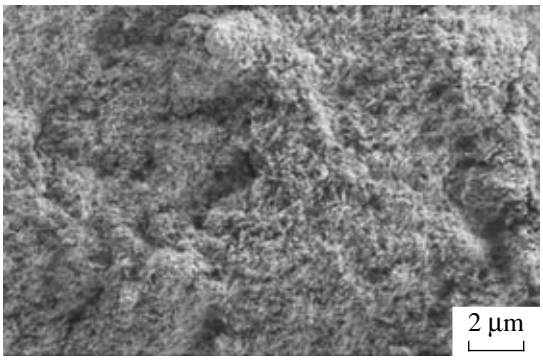

Fig. 3. SEM image of radial cross section of fresh Pt/γ-Al_2O_3 catalyst.

2.6.1. Characterization of silicon distribution in the spent pellets. The bulk silicon analyses were carried out using an ARL 3560 ICP-AES (Inductively Coupled Plasma-Atomic Emission Spectroscopy) instrument. For each analysis, the sample was ignited at 1000°C for 1 h. Then 0.125 g of the ignited sample was smelted with 0.375 g $LiBO_2$ and dissolved in HNO_3. This sample was then used to run ICP-AES.

The radial distribution of silicon in individual pellets was analyzed using a JEOL scanning electron microscope (model JXA-8600) equipped with an electron microprobe, operating in the wavelength dispersive mode (WDS). The deactivated cylindrical pellets were impregnated with epoxy resin using a vacuum impregnation unit. After that, they were cut radially, polished, and coated with an approximately 200 Å-thick carbon layer, and their cross sections were scanned along their diagonal.

3. RESULTS

3.1. BET Results

Table 4 shows the surface area and pore volume of fresh and deactivated samples. The result reveals that the specific surface areas of the top fraction of the blank support and Pt/γ-Al_2O_3 samples decrease somewhat after prolonged exposure to HMDS. The decrease in specific surface area is slightly more pronounced for the blank support than for the Pt/γ-Al_2O_3 sample.

3.2. Morphological Observation

An attempt was made to use SEM imaging to observe any probable morphological change of aged catalysts. The fresh Pt/γ-Al_2O_3 pellet and two top frac-

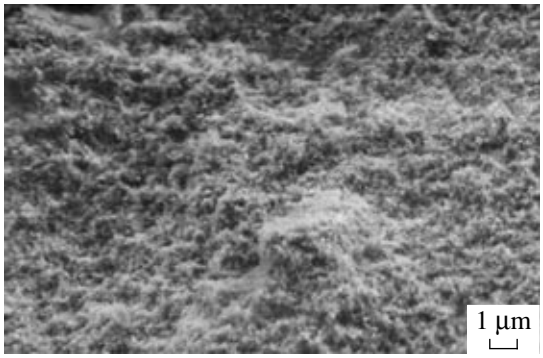

Fig. 4. SEM image of radial cross section of top fraction, 1000-h-aged Pt/γ-Al_2O_3 catalyst.

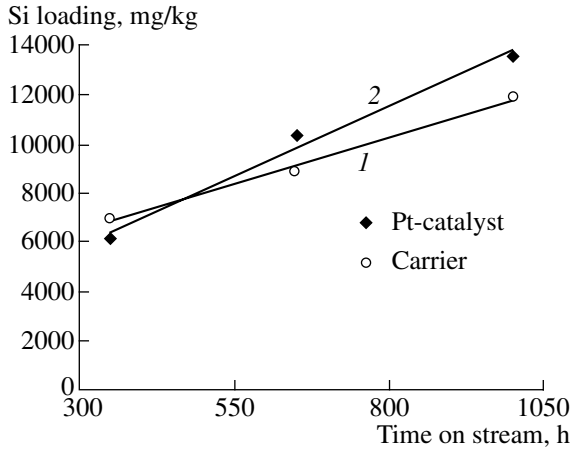

Fig. 5. Comparison of silicon loading for top fraction, γ-Al_2O_3 and Pt/γ-Al_2O_3.

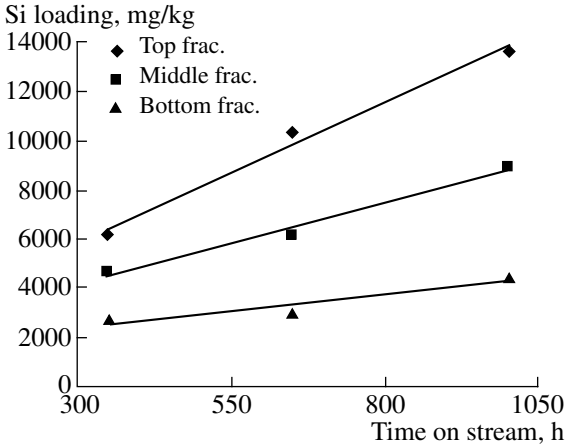

Fig. 6. Average silicon loading on Pt/γ-Al_2O_3 catalyst versus HMDS exposure time.

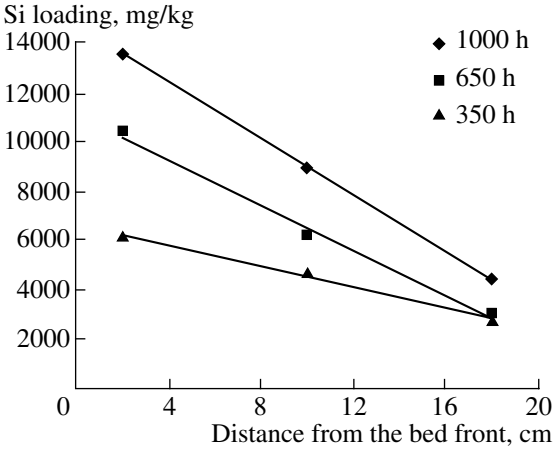

Fig. 7. Average silicon loading on Pt/γ-Al_2O_3 catalyst along the bed.

tions (samples aged for 650 and 1000 h) were analyzed. The secondary electron imaging and backscattered electron imaging were performed and compared. Figures 3 and 4 show the secondary electron imaging of fresh and 1000-h-aged Pt/γ-Al_2O_3 pellets. No contaminated layer or morphological change in the Pt/γ-Al_2O_3 pellets could be revealed on a macroscale by SEM.

3.3. Bulk Silicon Analyses

3.3.1. Silicon loading on the catalyst and the blank support. The silicon loadings for the catalyst (Pt/γ-Al_2O_3) and the blank support (γ-Al_2O_3) are shown in Fig. 5. The results reveal that silicon deposition on the blank support has the same pattern and order of magnitude compared to platinum-supported one. For both pellets, the silicon loading shows a linear relationship with time, while it seems to be somewhat faster for Pt/γ-Al_2O_3 than for the blank support.

3.3.2. Silicon loading versus HMDS exposure time. Figure 6 shows the silicon loadings for different fractions of aged catalyst as a function of HMDS exposure time. Comparison between the amounts of silicon passed per each reactor tube and the average amounts of deposited silicon reveals that more than 64% of the silicon was deposited for 350-h-aged pellets. This value is 49.4 and 44.5% for 650- and 1000-h-aged pellets, respectively. The linear relationship between the amount of deposited silicon and HMDS exposure time can be seen for all catalyst fractions.

3.3.3. Silicon profile along the bed. The silicon loading as a function of axial position in the bed, i.e., distance from the reactor inlet, is presented in Fig. 7. Observation of a linear silicon profile along the bed is highly interesting. One notes that the silicon loading is linear not only with HMDS exposure time, but also with the axial position in the bed. The maximum silicon loading can be found at the reactor inlet and it increases with the HMDS exposure time.

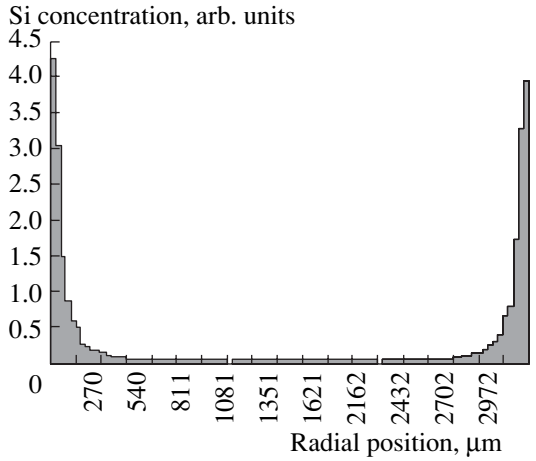

Fig. 8. Radial distribution of silicon in a single pellet, top fraction, 650 h deactivated.

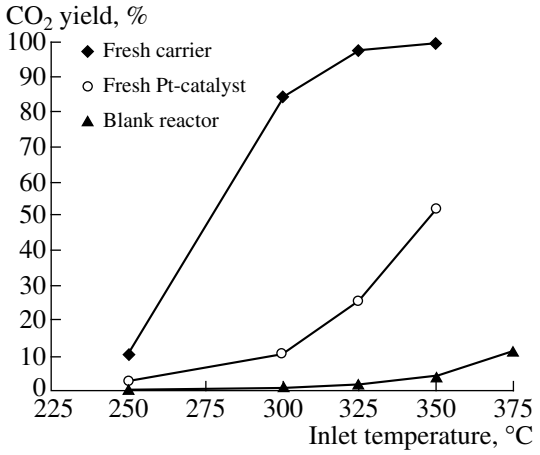

Fig. 9. Activity of fresh pellets and homogeneous oxidation in the blank reactor.

3.4. Silicon Profile in a Single Pellet

Figure 8 shows the radial distribution of silicon in an individual Pt/γ-Al_2O_3 pellet. The pellet was taken from a sample of the top fraction, which was exposed to HMDS for 650 h. The concentration scans along the pellet diagonal indicate a maximum silicon concentration at the outer surface of the pellet, which decreases toward the center. At a depth of about 500 μm, the silicon concentration is almost zero. This penetration depth reveals that silicon penetrated beyond the active phase zone.

3.5. Activity Data

3.5.1. Activity of fresh pellets and the effect of blank reactor. The fresh Pt/γ-Al_2O_3 shows a high activity for total oxidation of ethyl acetate at temperatures greater than 300°C. The temperature for 98% conversion to CO_2 (T_{98}) is around 325°C. At temperatures above 350°C, the CO_2 yield is more than 99.99% (Fig. 9). Formation of partial oxidation products on Pt/γ-Al_2O_3 catalyst has been investigated at different temperatures by comparing the CO_2 yield and total hydrocarbon conversion. It was observed that, at low temperatures, i.e., less than 275°C, a considerable amount of ethyl acetate is converted to partial oxidation products. The same results have been reported by Sawyer [19]. As temperature and, consequently, ethyl acetate conversion increase, CO_2 becomes the major product. At 300°C, almost all ethyl acetate undergoes a total oxidation reaction and is converted to CO_2. Figure 9 also shows the activity of γ-Al_2O_3 for the total oxidation of ethyl acetate. The CO_2 yield is about 52% at 350°C. For bare alumina support, the partial oxidation can be seen even at 325°C. However, as temperature increases, the CO_2 becomes the dominant product. No considerable partial oxidation products were observed at 350°C.

Table 5. Comparison of ethyl acetate total oxidation at 300°C over Pt/γ-Al_2O_3

Catalyst, Pt/γ-Al_2O_3	CO_2 yield, %	Percent decrease in CO_2 yield
Fresh	84	–
350 h deactivated, top frac.	80	4.8
650 h deactivated, top frac.	71	15.5
1000 h deactivated, top frac.	62	26.2

A blank experiment in an empty reactor was conducted to study the contribution of homogeneous oxidation of ethyl acetate. The hydrocarbon conversion in the gas phase was negligible. The CO_2 yield was around 4% at 350°C and 11% at 375°C, the highest temperature investigated here.

3.5.2. Effect of HMDS exposure time. The effects of hexamethyldisiloxane exposure time on the activity of Pt/γ-Al_2O_3 catalyst for the total oxidation of ethyl acetate are presented in Figs. 10 and 11. A similar behavior can be seen for different fractions of catalyst in the bed. With increasing exposure time, the CO_2 yield decreases. There is a significant difference in catalyst activity at 300°C. Table 5 summarizes the activity loss for aged Pt/γ-Al_2O_3 catalyst for the top fractions at 300°C. The highest deactivation level was observed for 1000-h-aged pellets.

In practice, the required temperature to obtain 98% conversion (T_{98}) is a significant indication of deactivation of VOC abatement catalysts. This value has been calculated for all aged Pt/γ-Al_2O_3 top fractions. While T_{98} is 325°C for the fresh catalyst, it increases to 350, 375, and 380°C (extrapolated) for 350-, 650-, and 1000-h-aged pellets, respectively.

3.5.3. Activity profile along the bed. To study the activity profile of catalyst along the bed, different fractions with the same HMDS exposure time have been

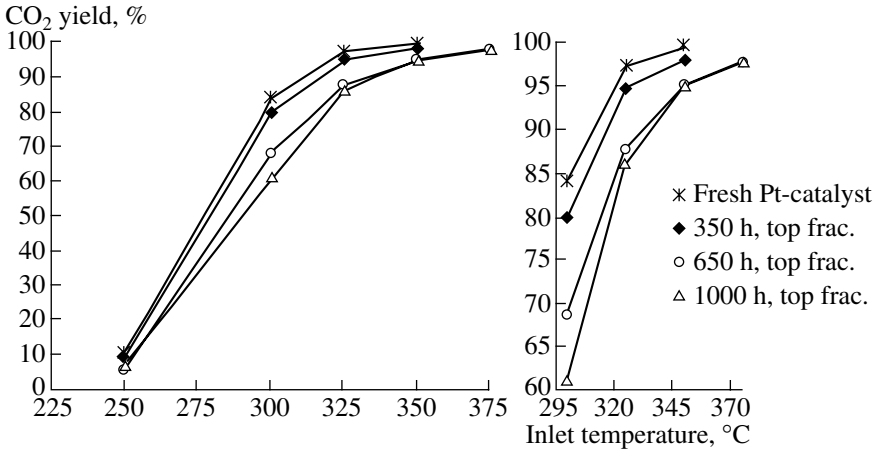

Fig. 10. Effect of HMDS exposure time on the total oxidation of ethyl acetate over aged Pt/γ-Al_2O_3 catalyst, top fractions.

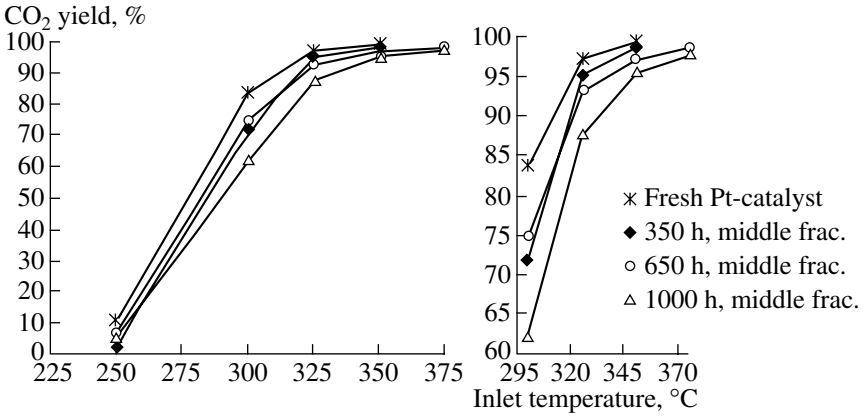

Fig. 11. Effect of HMDS exposure time on the total oxidation of ethyl acetate over aged Pt/γ-Al_2O_3 catalyst, middle fractions.

tested using the standard set of operating conditions in Table 3. The results are plotted in Figs. 12 and 13. These figures show a small difference in catalytic activity along the bed. Comparing the CO_2 yield of the top fraction to the bottom fraction varies with a maximum difference of about 5%.

3.5.4. Activity of the aged γ-Al_2O_3. The effect of HMDS on the activity of blank support (γ-Al_2O_3) is presented in Fig. 14. Alumina is well known to promote partial oxidation, hydration, rearrangement, and dehydrogenation [19]. However, it seems that silicon deposition on the γ-Al_2O_3 surface suppresses its activity. A drastic decrease (64%) in CO_2 yield can be seen at 350°C. The loss in activity is reduced as temperature decreases. The same behavior was observed in the case of total hydrocarbon conversion.

4. DISCUSSION

4.1. Catalyst Behavior Toward HMDS Exposure

Both the Pt/γ-Al_2O_3 catalyst and the blank support were deactivated as they were exposed to HMDS. Bulk silicon analyses confirmed that the silicon residues were deposited as a result of the interaction of organosilicon with precious metal and alumina surfaces. From BET analysis, it seems that the silicon deposition leaves the average surface area almost intact or with minor changes. While the pores of the catalyst can indeed be

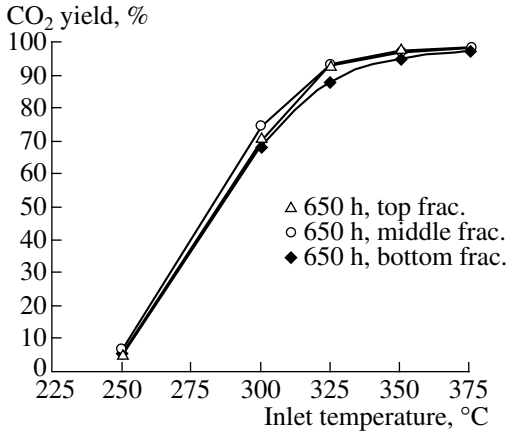

Fig. 12. Activity profile along the bed for 650-h-aged Pt/γ-Al_2O_3 catalyst.

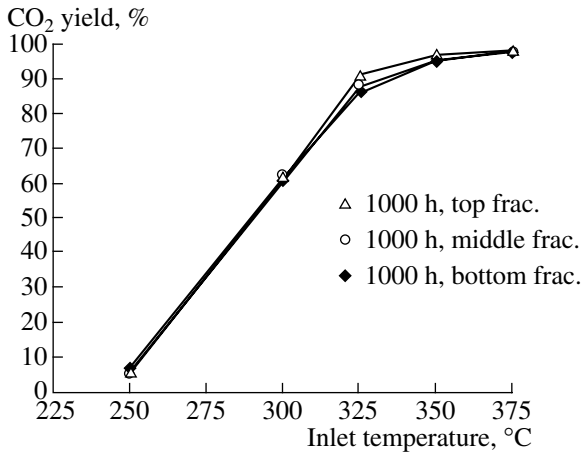

Fig. 13. Activity profile along the bed for 1000-h-aged Pt/γ-Al_2O_3 catalyst.

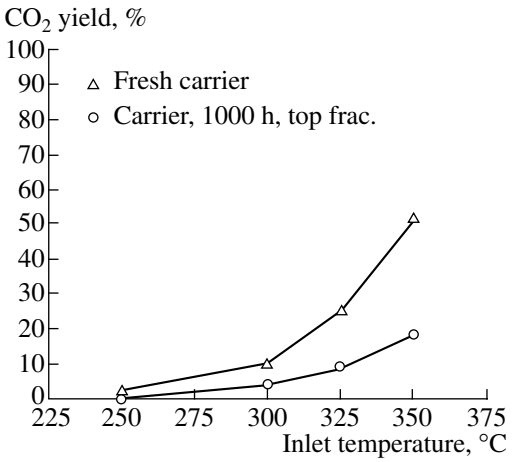

Fig. 14. Effect of HMDS on the activity of blank support (γ-Al_2O_3).

obstructed by poisonous deposits in certain instances [20], such a process apparently did not occur in the experiments reported here. Negligible morphological changes indicate that the silicon residues were deposited in the form of a very thin overlayer on the surface of deactivated catalyst. Similar results have been reported for phosphorous accumulation in an accelerated aging test of automotive catalysts [21].

To understand the catalytic behavior of the fresh and the aged Pt/γ-Al_2O_3 catalyst in the total oxidation of ethyl acetate, a pseudo-first-order reaction model has been employed [22]. This macrokinetic model is based on the following assumptions: (1) isothermal operation; (2) ideal plug flow reactor; (3) ideal gas behavior; (4) negligible change in the gas volume due to reaction; and (5) first-order reaction for ethyl acetate conversion to CO_2:

$$k = -S\ln(1 - Y), \tag{3}$$

where k is the pseudo-first-order reaction rate constant (s^{-1}), S is the space velocity under the reaction conditions (s^{-1}), and Y is the conversion of ethyl acetate to carbon dioxide (CO_2 yield).

The rate constants for the fresh and aged Pt/γ-Al_2O_3 catalysts at 325 and 350°C are presented in Table 6. The rate constant and, consequently, the pseudo-first-order reaction rate for the fresh catalyst are about two times greater than that of the 1000-h HMDS-treated one. In addition, the activities of the spent catalysts decrease with HMDS exposure time. These results reveal that the effect of HMDS exposure time on the first two fractions of 350- and 650-h-aged pellets is much more profound than the other.

Table 6. Pseudo-first-order rate constants for Pt/γ-Al_2O_3 catalyst at 325 and 350°C

Catalyst, Pt/γ-Al_2O_3	k (s^{-1}) at 325°C	k (s^{-1}) at 350°C
Fresh	23.17	34.37
350 h deactivated, top frac.	18.86	26.73
650 h deactivated, top frac.	13.47	20.17
1000 h deactivated, top frac.	12.66	20.07

The conversion at low temperature can be used to determine the intrinsic activity, while the conversion at temperatures where mass transfer is limiting will determine the available active geometric surface needed for hydrocarbon oxidation [23]. Inspecting the activity data of fresh and aged pellets as a function of temperature in Figs. 10 and 11 reveals a considerable activity loss around 300°C, where the reaction rate is more kinetically controlled. At high temperatures (350°C or above) where mass transfer is limiting, the activity of aged pellets approaches their initial values. Moreover, inspecting the activity data of aged γ-Al_2O_3 shows that the alumina is deactivated for both total and partial oxidation reactions. All of these pieces of evidence support the above idea of surface coverage by a thin overlayer deposition of silicon residues, which prevents the gas molecules from reaching the surface sites.

Considering the bulk silicon profile along the bed, one can expect a considerable change in catalytic activity. Comparing the results for different fractions of 650- and 1000-h-aged pellets apparently shows a small variation. It seems that the HMDS exposure time has more severe effects than the silicon loading. In the previous studies, it was concluded that HMDS exposure to platinum-supported catalyst results in either reversible or irreversible deactivation, depending on the type of hydrocarbons [4, 5]. In the reversible cases, the activity was regained whenever HMDS was removed from the reactor feed. Apparently, in this work, the removal of HMDS from feed in the ex situ activity measurement tests caused a partial activity regaining. This may be

another reason for observing such a small variation in activity along the bed.

4.2. Silicon Deposition Phenomena

Analysis of silicon loadings for Pt/γ-Al_2O_3 samples and the blank support revealed that the silicon deposition on the catalyst surface is not dependent on the presence of an active metal component over the alumina support. It seems that organosilicon interacts with both the support and the active component (Pt). The silicon uptake is linear with time and somewhat faster for Pt/γ-Al_2O_3 than for the blank support, which suggests the promoting effect of platinum on deposition of silicon species on the catalyst surface [10]. The data also showed a linear silicon profile along the bed. The slope of this line increases with the time on stream. Such a phenomenon may indicate that silicon deposits preferentially at the upper sections of the reactor.

Inspecting the silicon profile inside an individual catalyst pellet shows a sharp gradient, with a maximum concentration of deposited silicon species at the outer surface of the pellet. This nonuniform distribution of deposits is an indication of the large ratio of the surface reaction rate to the rate of diffusion through the porous catalyst pellet, known as the Thiele modulus. A Thiele modulus very much smaller than unity results in a uniform deposition of poison species, while a Thiele modulus much larger than unity indicates a nonuniform shell-like deposition [24]. It seems that, in the case of silicon poisoning, the reactions leading to the deposits are fast (and the diffusion rates within the pores are relatively slow) and, as such, nonuniform deposition takes place. This is a so-called diffusion-controlled poison depositing process.

In a related work [25], using X-ray photoelectron spectroscopy (XPS), it was found that the silicon species are deposited on the catalyst surface as silicate (Si_xO_y, except SiO_2). It was postulated that HMDS adsorbs on the surface of the catalyst and decomposes with the cleavage of the Si-CH_3 bonds [5, 11]. Silicate is formed as silicon binds to the surface through oxygen bridges. HMDS also adsorbs and decomposes on alumina, but to a lesser extent compared to the more catalytically active platinum surfaces. The silicate will first deposit as a monolayer; nevertheless, with increasing HDMS exposure, multilayer structures will be formed as well.

One interesting aspect of the silicon deposition phenomenon is that about 50% of the total silicon present in the reactor feed passed through the reactor without being deposited. Considering the very small amount of HMDS in the feed and that a strong oxidative environment prevailed within the reactor, it seems that there was not enough driving force to capture such a minute amount of silicon and, in addition, the driving force was decreased with increasing HMDS exposure time. It was not possible, however, to identify the nature of this leaving silicon species through this work.

It is worth noting that, within the time scale of the slow pilot aging experiments performed here, the silicon profile is linear versus both HMDS exposure time and the axial position in the reactor. A comparison between these results and those obtained from the field-aged catalysts [6] shows a smaller gradient in the silicon profile along the bed. The probable reasons could be the higher poison concentration utilized in the pilot experiment and the shorter exposure time. Owing to the employment of these modified experimental conditions, care has to be taken when extrapolating the results to a real application.

5. CONCLUSIONS

On the time scale of the aging experiments reported here, the following conclusions may be drawn: (1) Silicon residues deposited on both the Pt/γ-Al_2O_3 catalyst and the blank support. (2) The silicon profile along the bed is linear and decreasing, which indicates the silicon residues preferentially deposited at the reactor inlet. (3) The silicon loading versus HMDS exposure time is again linear. It is also faster for Pt/γ-Al_2O_3, which indicates the promoting effect of platinum. (4) About 50% of the total silicon present in the reactor feed passed through the reactor without being deposited. (5) No considerable change in surface area and pore volumes was observed. (6) From a macroscopic point of view, silicon residues deposited in the form of very thin overlayers covering and blocking the surface sites. (7) The radial silicon distribution in individual pellets showed an eggshell distribution, which is an indication of a diffusion-limited mechanism of silicon deposition. (8) None of the aged catalysts could convert ethyl acetate to a sufficiently high degree in the operating window (325–350°C) of fresh Pt/γ-Al_2O_3 pellets. (9) The T_{98} parameter increased by 55°C for the 1000-h-aged top fraction of Pt/γ-Al_2O_3 catalyst.

It is of great importance to note that the results presented in this work are based on ex situ measurements. Using in situ activity measurements showed that aged catalysts could regain their activity after removing HMDS from the reactor feed. A detailed description of this phenomenon has been given by us elsewhere [26].

ACKNOWLEDGMENTS

The financial support from the Ministry of Science, Research, and Technology of Iran is gratefully acknowledged.

REFERENCES

1. Spivey, J.J. and Butt, J.B., *Catal. Today*, 1992, vol. 11, no. 4, p. 465.
2. Neyestanaki, A.K., Klingstedt, F., Salmi, T., et al., *Fuel*, 2004, vol. 83, nos. 4–5, p. 395.

3. Hegedus, L.L. and McCabe, R.W., *Catalyst Poisoning*, New York: Marcel Dekker, 1984.
4. Gentry, S.J. and Jones, A., *J. Appl. Chem. Biotechnol.,* 1978, vol. 28, no. 11, p. 727.
5. Cullis, C.F. and Willatt, B.M., *J. Catal.*, 1984, vol. 86, no. 1, p. 187.
6. Libanati, C., Ullenius, D.A., and Pereira, C.J., *Appl. Catal., B*, 1998, vol. 15, nos. 1–2, p. 21.
7. Rahmani, M., Sohrabi, M., Augustsson, O., et al., *53rd Canadian Chemical Engineering Conference*, Hamilton, Canada, 2003, paper no. 141.
8. Rahmani, M., Cruise, N., Sohrabi, M., et al., *XVI Int. Conf. on Chemical Reactors*, Berlin, 2003, p. 246.
9. Chilton, J.E., Baran, J.N., Thomas, W.E., et al., *Rock Mech.*, 1978, vol. 19, p. 17.
10. Colin, L., Cassuto, A., Ehrhardt, J.J., et al., *Appl. Surf. Sci.*, 1996, vol. 99, no. 3, p. 245.
11. Ehrhardt, J.J., Colin, L., and Jamois, D., *Sens. Actuators, B*, 1997, vol. 40, nos. 2–3, p. 117.
12. Matsumiya, M., Shin, W., Qiu, F., et al., *Sens. Actuators, B*, 2003, vol. 96, no. 3, p. 516.
13. Kellberg, L., Zeuthen, P., and Jakobsen, H.J., *J. Catal.*, 1993, vol. 143, no. 1, p. 45.
14. Souza, M.O.G, Reyes, P, and Rangel, M.C, in *Catalyst Deactivation*, Delmon, B. and Froment, C.F., Eds., Amsterdam: Elsevier, 1999, p. 469.
15. Rahmani, M, Badii, K, Faghihi, M, et al., in *Catalysis*, Spivey, J.J., and Roberts, G.W., Eds., Cambridge: Royal Society of Chemistry, 2004, vol. 17, p. 210.
16. Papageorgiou, P., Price, D.M., Gavriilidis, A., et al., *J. Catal.*, 1996, vol. 158, no. 2, p. 439.
17. Rahmani, M., *Ph.D. Dissertation*, Tehran: Amirkabir University of Technology, 2005.
18. Barret, E.P., Joyner, L.G., and Halenda, P.P., *J. Am. Chem. Soc.*, 1951, vol. 73, no. 3, p. 373.
19. Sawyer, J.E. and Abraham, M.A., *Ind. Eng. Chem. Res.*, 1994, vol. 33, no. 9, p. 2084.
20. Hegedus, L.L. and Cavendish, J.C., *Ind. Eng. Chem. Fundam.*, 1997, vol. 16, no. 3, p. 365.
21. Hegedus, L.L. and Baron, K., *J. Catal.*, 1978, vol. 54, no. 2, p. 115.
22. Butt, J.B., *Reaction Kinetics and Reactor Design*, New York: Marcel Dekker, 1999.
23. Chen, J., Heck, R.M., and Farrauto, R.J., *Catal. Today*, 1992, vol. 11, p. 517.
24. Butt, J.B. and Petersen, E.E., *Activation, Deactivation, and Poisoning of Catalysts*, San Diego: Academic, 1988.
25. Arnby, K., Rahmani, M., Sanati, M., et al., *Appl. Catal., B*, 2004, vol. 54, no. 1, p. 1.
26. Rahmani, M. and Sohrabi, M., submitted for publication in *Catal Lett*., 2005.